Advances in Materials Research, *Vol. 8, No. 4 (2019) 313-335*
DOI: https://doi.org/10.12989/amr.2019.8.4.313

Static and free vibration behavior of functionally graded sandwich plates using a simple higher order shear deformation theory

Nafissa Zouatnia*[1,2] and Lazreg Hadji[3,4]

[1] *Department of Mechanical Engineering, University of Tiaret, BP 78 Zaaroura, Tiaret, 14000, Algeria*
[2] *Laboratory of Structures, Geotechnics and Risks (LSGR), Hassiba Benbouali University of Chlef, BP 151, Hay Essalam, UHB Chlef, Chlef, 02000, Algeria*
[3] *Laboratory of Geomatics and Sustainable Development, University of Tiaret, 14000, Algeria*
[4] *Department of Mechanical Engineering, University of Tiaret, BP 78 Zaaroura, Tiaret, 14000, Algeria*

(*Received January 5, 2020, Revised January 23, 2020, Accepted February 1, 2020*)

Abstract. The objective of the present paper is to investigate the bending and free vibration behavior of functionally graded material (FGM) sandwich rectangular plates using an efficient and simple higher order shear deformation theory. Unlike other theories, there are only four unknown functions involved, as compared to five in other shear deformation theories. The most interesting feature of this theory is that it does not require the shear correction factor. Two common types of FGM sandwich plates are considered, namely, the sandwich with the FGM facesheet and the homogeneous core and the sandwich with the homogeneous facesheet and the FGM core. The equation of motion for the FGM sandwich plates is obtained based on Hamilton's principle. The closed form solutions are obtained by using the Navier technique. A static and free vibration frequency is given for different material properties. The accuracy of the present solutions is verified by comparing the obtained results with the existing solutions.

Keywords: sandwich; bending; free vibration; functionally graded plate; navier solution

1. Introduction

In recent years, the application of functionally graded (FG) sandwich structures in aerospace, marine, civil construction is growing rapidly due to their high strength-to-weight ratio. There exist two common types: sandwich structures with FG core and sandwich structures with FG skins. With the wide application of FG sandwich structures, understanding static and vibration of FG sandwich structures becomes an important task. Several researchers have developed different computational models and carried out static and dynamic analyses of FGM structures. Zenkour (2005) studied the static response of FGM sandwich plates subjected to sinusoidal load employing different plate theories. Li *et al*. (2008) studied free vibration of FGM sandwich rectangular plates with simply supported and clamped edges using the Ritz method. Zenkour and Alghamdi (2008) developed a unified shear deformable plate and performed thermoelastic bending analysis of FGM

*Corresponding author, Ph.D., E-mail: had_laz@yahoo.fr

http://www.techno-press.org/?journal=amr&subpage=5 ISSN: 2234-0912 (Print), 2234-179X (Online)

sandwich plate. Amirani *et al*. (2009) used the element free Galerkin method for free vibration analysis of sandwich beam with FG core. Naves *et al*. (2012) studied the static analysis of functionally graded sandwich plates according to a hyperbolic theory considering Zig-Zag and warping effects. Akbaş (2015a) studied the wave propagation of a functionally graded beam in thermal environments. Steel and Composite Structures. Akbaş (2015b) investigated the free vibration and bending of functionally graded beams resting on elastic foundation. Akbaş (2015c) analyze the post-buckling of axially functionally graded three-dimensional beams. Thai *et al*. (2016) presented a new simple shear and normal deformations theory for static, dynamic and buckling analyses of functionally graded material (FGM) isotropic and sandwich plates. Belarbi *et al*. (2016) developed a 2D isoparametric finite element model based on the layerwise approach for the Bending analysis of sandwich plates. Akbaş (2017a) developed the vibration and static analysis of functionally graded porous plates. Akbaş (2017b) used the generalized differantial quadrature method for the stability of a non-homogenous porous plate. Akbaş (2017c) analyze the nonlinear static of functionally graded porous beams under thermal effect. Akbaş (2017d) analyze the forced vibration of functionally graded nanobeams. Mirza *et al*. (2018) studied the effect of boundary conditions on the non-linear forced vibration response of isotropic plates. Akbaş (2018) analyze the Geometrically nonlinear of functionally graded porous beams. Nazargah and Meshkani (2018) used an efficient partial mixed finite element model for static and free vibration analyses of FGM plates rested on two-parameter elastic foundations. Balubaid *et al*. (2019) developed the free vibration investigation of FG nanoscale plate using nonlocal two variables integral refined plate theory. Belbachir *et al*. (2019) analyze the bending of anti-symmetric cross-ply laminated plates under nonlinear thermal and mechanical loadings. Sahla *et al*. (2019) studied the free vibration analysis of angle-ply laminated composite and soft core sandwich plates. Draiche *et al*. (2019) analyze the static of laminated reinforced composite plates using a simple first-order shear deformation theory. Abualnour *et al*. (2019) used a new four variable trigonometric refined plate theory the the thermomechanical analysis of antisymmetric laminated reinforced composite plates. Alimirzaei *et al*. (2019) investigated the nonlinear analysis of viscoelastic micro-composite beam with geometrical imperfection using FEM: MSGT electro-magneto-elastic bending, buckling and vibration solutions. Berghouti *et al*. (2019) analyze the vibration of nonlocal porous nanobeams made of functionally graded material. Chaabane *et al*. (2019) developed an analytical study of bending and free vibration responses of functionally graded beams resting on elastic foundation. Medani *et al*. (2019) studied the static and dynamic behavior of (FG-CNT) reinforced porous sandwich plate. Semmah *et al*. (2019) analyze the thermal buckling of SWBNNT on Winkler foundation by non local FSDT. Draoui *et al*. (2019) used the FSDT for the static and dynamic behavior of nanotubes-reinforced sandwich plates. Tlidji *et al*. (2019) analyze the vibration of different material distributions of functionally graded microbeam. Adda Bedia *et al*. (2019) used a new Hyperbolic Two-Unknown Beam Model for bending and buckling analysis of a nonlocal strain gradient nanobeams. Bourada *et al*. (2019) investigated the dynamic of porous functionally graded beam using a sinusoidal shear deformation theory. Boussoula *et al*. (2020) used a simple nth-order shear deformation theory for thermomechanical bending analysis of different configurations of FG sandwich plates. Meksi *et al*. (2019) developed an analytical solution for bending, buckling and vibration responses of FGM sandwich plates. Hellal *et al*. (2019) analyze the dynamic and stability of functionally graded material sandwich plates in hygro-thermal environment using a simple higher shear deformation theory. Hussain *et al*. (2019) studied the nonlocal effect on the vibration of armchair and zigzag SWCNTs with bending rigidity. Karami *et al*. (2019a) used the Galerkin's approach for buckling analysis of functionally graded anisotropic nanoplates/different boundary conditions. Karami *et al*. (2019b) studied the wave propagation of functionally graded anisotropic nanoplates resting on Winkler-Pasternak foundation. Karami *et al*. (2019c) investigated the resonance behavior of functionally graded polymer composite nanoplates reinforced with grapheme nanoplatelets. Karami *et al*. (2019d) analyze the exact wave propagation of triclinic material using three dimensional bi-Helmholtz gradient plate model. Karami *et al*. (2019e) studied the pre stressed functionally graded anisotropic nanoshell in magnetic field. Kaddari *et al*. (2020) studied the structural behaviour of functionally graded porous plates on elastic foundation using a new quasi-3D model: bending and free vibration analysis. In addition, in recent years, many researchers have dealt the effect of stretching the thickness on FGM structures (Addou *et al*. 2019, Boutaleb *et al*. 2019, Khiloun *et al*. 2019, Zarga *et al*. 2019, Boulefrakh *et al*. 2019, Boukhlif *et al*. 2019, Mahmoudi *et al*. 2019, Zaoui *et al*. 2019).

Recently, Cunedioglu (2015) analyze the free vibration analysis of edge cracked symmetric functionally graded sandwich beams. Arani *et al*. (2017) studied theoretical investigation on vibration frequency of sandwich plate with PFRC core and piezomagnetic face sheets under variable in-plane load. Abdelaziz *et al*. (2017) used an efficient hyperbolic shear deformation theory for bending, buckling and free vibration of FGM sandwich plates with various boundary conditions. Shashank and Pradyumna (2018) used a higher-order layerwise theory for functionally graded sandwich plates. Abazid *et al*. (2018) used a novel shear and normal deformation theory for hygrothermal bending response of FGM Sandwich plates on Pasternak elastic foundation. Ahmadi (2018) studied the three-dimensional and free-edge hygrothermal stresses in general long Sandwich plates. Dash *et al*. (2018) investigated modal of FG sandwich doubly curved shell structure. Sudhakar *et al*. (2018) developed of super convergent euler finite elements for the analysis of sandwich beams with soft core. Dash *et al*. (2018) developed modal of FG sandwich doubly curved shell structure. Kolahdouzan *et al*. (2018) analyze of buckling and free vibration of FG-CNTRC-micro sandwich plate. Akbaş (2019) studied the forced vibration analysis of functionally graded sandwich deep beams. Mahmoud *et al*. (2019) analyze the thermodynamic behavior of functionally graded sandwich plates resting on different elastic foundation and with various boundary conditions.

In the present study, the bending and free vibration of the FGM sandwich plates is investigated using the four-variable refined plate theory. The most interesting feature of this theory is that it does not require the shear correction factor. Two common types of FGM sandwich plates, namely, the sandwich with the FGM facesheet and the homogeneous core and the sandwich with the homogeneous facesheet and the FGM core, are considered. The present theory satisfies equilibrium conditions at the top and bottom faces of the sandwich plate. The Navier solution is used to obtain the closed form solutions for simply supported FGM sandwich plates. Numerical examples are presented to verify the accuracy of the present theory. Final conclusions are presented in Section 6.

2. Problem formulation

2.1 Geometrical configuration

Consider the case of a rectangular FGM sandwich plate with the uniform thickness composed of three microscopically heterogeneous layers referring to rectangular coordinates (x, y, z) as shown in Fig. 1. The top and bottom faces of the plate are at $z = \pm h/2$, and the edges of the plate are parallel to axes x and y. The plate is subjected to a transverse mechanical load applied at the

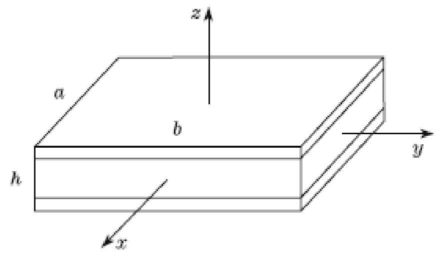

Fig. 1 Geometry of the rectangular FGM sandwich plate with uniform thickness in rectangular Cartesian coordinates

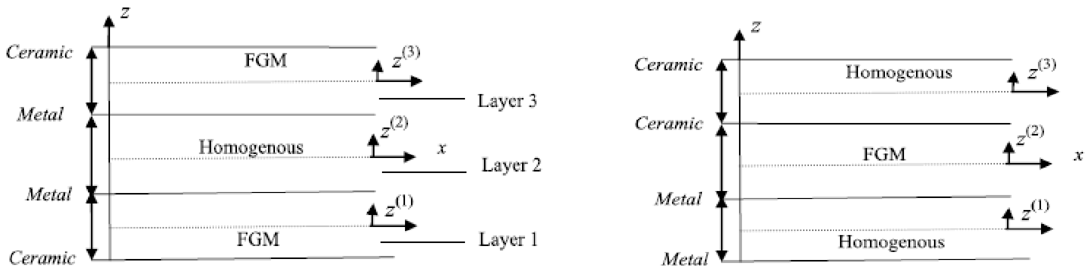

Fig. 2 Sandwich plate configurations: (a) Sandwich plate with FGM facesheets and homogenous core (Type A); (b) Sandwich plate with homogenous facesheets and FGM core (Type B)

top of the plate.

The sandwich plate is composed of three elastic layers, namely, Layer 1, Layer 2, and Layer 3 from bottom to top of the plate. The vertical ordinates of the bottom, the two interfaces, and the top are denoted by $\delta_0 = -h/2$, δ_1, δ_2, and h4 = h/2, respectively. For brevity, the ratio of the thicknes $\delta_3 = +h/2$ of each layer from bottom to top is denoted by the combination of three numbers, i.e., “1-0-1”, “2-1-2” and so on. As shown in Fig. 2, Types A and B are considered in the present study, i.e., the FGM facesheet and the homogeneous core and the homogeneous facesheet and the FGM core.

2.2 Rule of mixture

In the present study, material properties are estimated according to the rule of mixture. For Type A FGM sandwich plates, the effective material property like Young’s modulus $E^{(i)}$, and mass density $\rho^{(i)}$ for any ith layer is given as

$$P_{eff}^{(i)} = P_c + (P_m - P_c)\lambda^{(i)} \tag{1}$$

where Pm and Pc are material properties of pure metallic and ceramic constituents, respectively. $\lambda^{(i)}$ (i = 1, 2, 3) is the volume fraction of the metallic constituent for the ith layer of Type A FGM sandwich plate. The value of $\lambda^{(i)}$ lies between 0 and 1 and the variation of the same is given by

$$\lambda^{(1)} = \left(\frac{z - \delta_0}{\delta_1 - \delta_0}\right), \qquad z \in [\delta_0, \delta_1] \tag{2a}$$

$$\lambda^{(2)} = 1, \qquad z \in [\delta_1, \delta_2] \tag{2b}$$

$$\lambda^{(3)} = \left(\frac{z - \delta_3}{\delta_2 - \delta_3}\right), \qquad z \in [\delta_2, \delta_3] \tag{2c}$$

For Type B FGM sandwich plate, the effective material properties $E^{(i)}$, $\rho^{(i)}$ are obtained as

$$\lambda^{(1)} = 0, \qquad z \in [\delta_0, \delta_1] \tag{3a}$$

$$\lambda^{(2)} = \left(\frac{z - \delta_0}{\delta_1 - \delta_0}\right), \qquad z \in [\delta_1, \delta_2] \tag{3b}$$

$$\lambda^{(3)} = 1, \qquad z \in [\delta_2, \delta_3] \tag{3c}$$

2.3 Basic assumptions

The assumptions of the present theory are as follows:

- The displacements are small in comparison with the plate thickness. Therefore, the strains involved are infinitesimal.
- The transverse displacement w includes two components of bending w_b, and shear w_s. These components are functions of coordinates x, y and time t only.

$$w(x, y, z, t) = w_b(x, y, t) + w_s(x, y, t) \tag{4}$$

The transverse normal stress$\sigma_z$is negligible in comparison with in-plane stresses σ_x and σ_y.

- The axial displacement u in x-direction and v in the y-direction, consists of extension, bending, and shear components.

$$u = u_0 + u_b + u_s, \qquad v = v_0 + v_b + v_s \tag{5}$$

- The bending component u_b and v_b are assumed to be similar to the displacements given by the classical plate theory. Therefore, the expression for u_b and v_b can be given as

$$u_b = -z\frac{\partial w_b}{\partial x}, \qquad v_b = -z\frac{\partial w_b}{\partial y} \tag{6}$$

- The shear components u_s and v_s gives rise, in conjunction with w_s, to the hyperbolic variation of shear strains γ_{xz}, γ_{yz} and hence to shear stresses τ_{xz}, τ_{yz} through the thickness of the plate in such a way that shear stresses τ_{xz}, τ_{yz} are zero at the top and bottom faces of the plate. Consequently, the expression for u_s and v_s can be given as

$$u_s = -f(z)\frac{\partial w_s}{\partial x}, \qquad v_s = -f(z)\frac{\partial w_s}{\partial y} \tag{7}$$

where

$$f(z) = z - \frac{h}{\pi} sin\left(\frac{\pi z}{h}\right) \tag{8}$$

2.4 Kinematics and constitutive equations

Based on the assumptions made in the preceding section, the displacement field can be obtained using Eqs. (4)-(8) as

$$\begin{aligned} u(x,y,z) &= u_0(x,y,t) - z\frac{\partial w_b}{\partial x} - f(z)\frac{\partial w_s}{\partial x} \\ v(x,y,z) &= v_0(x,y,t) - z\frac{\partial w_b}{\partial y} - f(z)\frac{\partial w_s}{\partial y} \\ w(x,y,z) &= w_b(x,y) + w_s(x,y) \end{aligned} \tag{9}$$

The strains associated with the displacements in Eq. (9) are

$$\begin{aligned} \varepsilon_x &= \varepsilon_x^0 + z_{ns}\, k_x^b + f(z_{ns})\, k_x^s \\ \varepsilon_y &= \varepsilon_y^0 + z_{ns}\, k_y^b + f(z_{ns})\, k_y^s \\ \gamma_{yz} &= g(z_{ns})\, \gamma_{yz}^s \\ \gamma_{xz} &= g(z_{ns})\, \gamma_{xz}^s \\ \varepsilon_z &= 0 \end{aligned} \tag{10}$$

where

$$\begin{aligned} &\varepsilon_x^0 = \frac{\partial u_0}{\partial x}, \qquad k_x^b = -\frac{\partial^2 w_b}{\partial x^2}, \qquad k_x^s = -\frac{\partial^2 w_s}{\partial x^2}, \\ &\varepsilon_y^0 = \frac{\partial v_0}{\partial x}, \qquad k_y^b = -\frac{\partial^2 w_b}{\partial y^2}, \qquad k_y^s = -\frac{\partial^2 w_s}{\partial y^2}, \\ &\gamma_{yz}^s = \frac{\partial w_s}{\partial x}, \qquad \gamma_{xz}^s = \frac{\partial w_s}{\partial x}, \qquad g(z) = 1 - f'(z), \qquad f'(z) = \frac{df(z)}{dz} \end{aligned} \tag{11}$$

For elastic and isotropic FGMs, the constitutive relations can be written as

$$\begin{Bmatrix} \sigma_x \\ \sigma_y \\ \tau_{yz} \\ \tau_{xz} \\ \tau_{xy} \end{Bmatrix}^{(n)} = \begin{bmatrix} Q_{11} & Q_{12} & 0 & 0 & 0 \\ Q_{12} & Q_{22} & 0 & 0 & 0 \\ 0 & 0 & Q_{44} & 0 & 0 \\ 0 & 0 & 0 & Q_{55} & 0 \\ 0 & 0 & 0 & 0 & Q_{66} \end{bmatrix}^{(n)} \begin{Bmatrix} \varepsilon_x \\ \varepsilon_y \\ \gamma_{yz} \\ \gamma_{xz} \\ \gamma_{xy} \end{Bmatrix}^{(n)} \tag{12}$$

where

$$Q_{11}(z) = \frac{E(z)}{(1-\nu^2)}, \qquad Q_{12}(z) = \nu Q_{11}(z) \tag{13}$$

and

$$Q_{44}(z) = Q_{55}(z) = Q_{66}(z) = \frac{E(z)}{2(1+\nu)} \tag{14}$$

2.5 Governing equations

Using Hamilton's energy principle derives the equation of motion of the FG plate

$$\int_0^T (\delta\, U + \delta\, V - \delta\, T)dt = 0 \tag{15}$$

where δU is the variation of strain energy; δV is the variation of work done by external forces; and δT is the variation of kinetic energy. The variation of strain energy is calculated by

$$\begin{aligned}\delta U &= \int_{\Omega}\int_{-\frac{h}{2}}^{\frac{h}{2}}\left[\sigma_x\delta\,\varepsilon_x + \sigma_y\delta\,\varepsilon_y + \tau_{xy}\delta\,\gamma_{xy} + \tau_{yz}\delta\,\gamma_{yz} + \tau_{xz}\delta\,\gamma_{xz}\right]dzd\Omega \\ &= \int_{\Omega}\left[N_x\delta\,\varepsilon_x^0 + N_y\delta\,\varepsilon_y^0 + N_{xy}\delta\,\varepsilon_{xy}^0 + M_x^b\delta\,k_x^b + M_y^b\delta\,k_y^b + M_{xy}^b\delta\,k_{xy}^b + M_x^s\delta\,k_x^s\right. \\ &\quad \left.+M_y^s\delta\,k_y^s + M_{xy}^s\delta\,k_{xy}^s + S_{yz}^s\delta\,\gamma_{yz}^s + S_{xz}^s\delta\,\gamma_{xz}^s\right]d\Omega\end{aligned} \tag{16}$$

where Ω is the top surface and $N,\ M,$ and S are stress resultants defined by

$$\begin{Bmatrix} N_x, & N_y, & N_{xy} \\ M_x^b, & M_y^b, & M_{xy}^b \\ M_x^s, & M_y^s, & M_{xy}^s \end{Bmatrix} = \sum_{n=1}^{3}\int_{h_n}^{h_{n+1}}\left(\sigma_x,\sigma_y,\tau_{xy}\right)^{(n)}\begin{Bmatrix} 1 \\ z \\ f(z)\end{Bmatrix}dz \tag{17a}$$

$$\left(S_{xz}^s, S_{yz}^s\right) = \sum_{n=1}^{3}\int_{h_n}^{h_{n+1}}\left(\tau_{xz},\tau_{yz}\right)^{(n)}g(z)dz \tag{17b}$$

Where h_{n+1} and h_n are the top and bottom z-coordinates of the nth layer.
The variation of work done by external forces can be expressed as

$$\delta V = -\int_{\Omega} q(\delta\,w_b + \delta\,w_b)\,d\Omega \tag{18}$$

where q is the transverse load. The variation of kinetic energy can be written as

$$\begin{aligned}\delta T &= \int_{-\frac{h}{2}}^{\frac{h}{2}}\int_{\Omega}[\dot{u}\delta\,\dot{u} + \dot{v}\delta\,\dot{v} + \dot{w}\delta\,\dot{w}]\,\rho(z)\ d\Omega\ dz \\ &= \int_A\{I_0[\dot{u}_0\delta\dot{u}_0 + \dot{v}_0\delta\dot{v}_0 + (\dot{w}_b + \dot{w}_s)(\delta\dot{w}_b + \delta\dot{w}_s)] \\ &\quad -I_1\left(\dot{u}_0\frac{\partial\delta\dot{w}_b}{\partial x} + \frac{\partial\dot{w}_b}{\partial x}\delta\,\dot{u}_0 + \dot{v}_0\frac{\partial\delta\dot{w}_b}{\partial y} + \frac{\partial\dot{w}_b}{\partial y}\delta\,\dot{v}_0\right) \\ &\quad -J_1\left(\dot{u}_0\frac{\partial\delta\dot{w}_s}{\partial x} + \frac{\partial\dot{w}_s}{\partial x}\delta\,\dot{u}_0 + \dot{v}_0\frac{\partial\delta\dot{w}_s}{\partial y} + \frac{\partial\dot{w}_s}{\partial y}\delta\,\dot{v}_0\right) \\ &\quad +I_2\left(\frac{\partial\dot{w}_b}{\partial x}\frac{\partial\delta\,\dot{w}_b}{\partial x} + \frac{\partial\dot{w}_b}{\partial y}\frac{\partial\delta\,\dot{w}_b}{\partial y}\right) + K_2\left(\frac{\partial\dot{w}_s}{\partial x}\frac{\partial\delta\,\dot{w}_s}{\partial x} + \frac{\partial\dot{w}_s}{\partial y}\frac{\partial\delta\,\dot{w}_s}{\partial y}\right) \\ &\quad +J_2\left(\frac{\partial\dot{w}_b}{\partial x}\frac{\partial\delta\,\dot{w}_s}{\partial x} + \frac{\partial\dot{w}_s}{\partial x}\frac{\partial\delta\,\dot{w}_b}{\partial x} + \frac{\partial\dot{w}_b}{\partial y}\frac{\partial\delta\,\dot{w}_s}{\partial y} + \frac{\partial\dot{w}_s}{\partial y}\frac{\partial\delta\,\dot{w}_b}{\partial y}\right)\Bigg\}d\Omega\end{aligned} \tag{19}$$

Where dot-superscript convention indicates the differentiation with respect to the time variable t; and $(I_0,\ I_1,\ J_1,\ I_2,\ J_2,\ K_2)$ are mass inertias defined as

$$(I_0, I_1, J_1, I_2, J_2, K_2) = \sum_{n=1}^{3}\int_{h_n}^{h_{n+1}}(1, z, f, z^2, z\,f, f^2)\rho(z)dz \tag{20}$$

Substituting the expressions for δU, δV, and δT from Eqs. (16), (18), and (19) into Eq. (15) and integrating by parts, and collecting the coefficients of δu_0, δv_0, δw_b, and δw_s, one obtains the following equations of motion

$$\delta u_0:\ \frac{\partial N_x}{\partial x}+\frac{\partial N_{xy}}{\partial y}=I_0\ddot{u}_0-I_1\frac{\partial \ddot{w}_b}{\partial x}-J_1\frac{\partial \ddot{w}_s}{\partial x} \tag{21a}$$

$$\delta v_0:\ \frac{\partial N_{xy}}{\partial x}+\frac{\partial N_y}{\partial y}=I_0\ddot{v}_0-I_1\frac{\partial \ddot{w}_b}{\partial y}-J_1\frac{\partial \ddot{w}_s}{\partial y} \tag{21b}$$

$$\begin{aligned}\delta w_b:\ &\frac{\partial^2 M_x^b}{\partial x^2}+2\frac{\partial^2 M_{xy}^b}{\partial x\partial y}+\frac{\partial^2 M_y^b}{\partial y^2}+q\\ &=I_0(\ddot{w}_b+\ddot{w}_s)+I_1\left(\frac{\partial \ddot{u}_0}{\partial x}+\frac{\partial \ddot{v}_0}{\partial y}\right)-I_2\nabla^2\ddot{w}_b-J_2\nabla^2\ddot{w}_s\end{aligned} \tag{21c}$$

$$\begin{aligned}\delta w_s:\ &\frac{\partial^2 M_x^s}{\partial x^2}+2\frac{\partial^2 M_{xy}^s}{\partial x\partial y}+\frac{\partial^2 M_y^s}{\partial y^2}+\frac{\partial S_{xz}^s}{\partial x}+\frac{\partial S_{yz}^s}{\partial y}+q\\ &=I_0(\ddot{w}_b+\ddot{w}_s)+J_1\left(\frac{\partial \ddot{u}_0}{\partial x}+\frac{\partial \ddot{v}_0}{\partial y}\right)-J_2\nabla^2\ddot{w}_b-K_2\nabla^2\ddot{w}_s\end{aligned} \tag{21d}$$

Substituting Eq. (12) into Eq. (17) and integrating through the thickness of the plate, the stress resultants are given as

$$\begin{Bmatrix} N \\ M^b \\ M^s \end{Bmatrix}=\begin{bmatrix} A & 0 & B^s \\ 0 & D & D^s \\ B^s & D^s & H^s \end{bmatrix}\begin{Bmatrix} \varepsilon \\ k^b \\ k^s \end{Bmatrix},\quad S=A^s\gamma \tag{22}$$

where

$$N=\{N_x,N_y,N_{xy}\}^t,\ \ M^b=\{M_x^b,M_y^b,M_{xy}^b\}^t,\ \ M^s=\{M_x^s,M_y^s,M_{xy}^s\}^t, \tag{23a}$$

$$\varepsilon=\{\varepsilon_x^0,\varepsilon_y^0,\gamma_{xy}^0\}^t,\quad k^b=\{k_x^b,k_y^b,k_{xy}^b\}^t,\quad k^s=\{k_x^s,k_y^s,k_{xy}^s\}^t, \tag{23b}$$

$$A=\begin{bmatrix} A_{11} & A_{12} & 0 \\ A_{12} & A_{22} & 0 \\ 0 & 0 & A_{66} \end{bmatrix},\ A=\begin{bmatrix} B_{11} & B_{12} & 0 \\ B_{12} & B_{22} & 0 \\ 0 & 0 & B_{66} \end{bmatrix},\ D=\begin{bmatrix} D_{11} & D_{12} & 0 \\ D_{12} & D_{22} & 0 \\ 0 & 0 & D_{66} \end{bmatrix}, \tag{23c}$$

$$B^s=\begin{bmatrix} B_{11}^s & B_{12}^s & 0 \\ B_{12}^s & B_{22}^s & 0 \\ 0 & 0 & B_{66}^s \end{bmatrix},\ D^s=\begin{bmatrix} D_{11}^s & D_{12}^s & 0 \\ D_{12}^s & D_{22}^s & 0 \\ 0 & 0 & D_{66}^s \end{bmatrix},\ H^s=\begin{bmatrix} H_{11}^s & H_{12}^s & 0 \\ H_{12}^s & H_{22}^s & 0 \\ 0 & 0 & H_{66}^s \end{bmatrix}, \tag{23d}$$

$$S=\{S_{xz}^s,S_{yz}^s\}^t,\quad \gamma=\{\gamma_{xz},\gamma_{yz}\}^t,\quad A^s=\begin{bmatrix} A_{44}^s & 0 \\ 0 & A_{55}^s \end{bmatrix}, \tag{23e}$$

The stiffness coefficients A_{ij} and D_{ij}, etc., are defined as

$$\begin{Bmatrix} A_{11} & B_{11} & D_{11} & B_{11}^s & D_{11}^s & H_{11}^s \\ A_{12} & B_{12} & D_{12} & B_{12}^s & D_{12}^s & H_{12}^s \\ A_{66} & B_{66} & D_{66} & B_{66}^s & D_{66}^s & H_{66}^s \end{Bmatrix}=\sum_{n=1}^{3}\int_{h_n}^{h_{n+1}} Q_{11}^{(n)}(1,z,z^2,f(z),z\,f(z),f^2(z))\begin{Bmatrix} 1 \\ \nu^{(n)} \\ \dfrac{1-\nu^{(n)}}{2} \end{Bmatrix}dz \tag{24a}$$

$$(A_{22}, B_{22}, D_{22}, B_{22}^s, D_{22}^s, H_{22}^s) = (A_{11}, B_{11}, D_{11}, B_{11}^s, D_{11}^s, H_{11}^s) \tag{24b}$$

$$A_{44}^s = A_{55}^s = \sum_{n=1}^{3} \int_{h_n}^{h_{n+1}} \frac{E(z)}{2(1+\nu)} [g(z)]^2 dz \tag{24c}$$

By substituting Eq. (22) into Eq. (21), the equations of motion can be expressed in terms of displacements ($\delta\, u_0,\ \delta\, v_0,\ \delta\, w_b,\ \delta\, w_s$) as

$$\begin{aligned} &A_{11}\frac{\partial^2 u_0}{\partial x^2} + A_{66}\frac{\partial^2 u_0}{\partial y^2} + (A_{12}+A_{66})\frac{\partial^2 v_0}{\partial x \partial y} B_{11}\frac{\partial^3 w_b}{\partial x^3} \\ &-(B_{12}+2B_{66})\frac{\partial^3 w_b}{\partial x \partial y^2} - (B_{12}^s + 2B_{66}^s)\frac{\partial^3 w_s}{\partial x \partial y^2} - B_{11}^s\frac{\partial^3 w_s}{\partial x^3} \\ &= I_0 \ddot{u}_0 - I_1\frac{\partial \ddot{w}_b}{\partial x} - J_1\frac{\partial \ddot{w}_s}{\partial x} \end{aligned} \tag{25a}$$

$$\begin{aligned} &A_{22}\frac{\partial^2 v_0}{\partial y^2} + A_{66}\frac{\partial^2 v_0}{\partial x^2} + (A_{12}+A_{66})\frac{\partial^2 u_0}{\partial x \partial y} \\ &-\mathrm{B}_{22}\frac{\partial^3 w_b}{\partial y^3} - (B_{12}^s + 2B_{66}^s)\frac{\partial^3 w_s}{\partial x^2 \partial y} - B_{22}^s\frac{\partial^3 w_s}{\partial y^3} \\ &= I_0 \ddot{v}_0 - I_1\frac{\partial \ddot{w}_b}{\partial y} - J_1\frac{\partial \ddot{w}_s}{\partial y}, \end{aligned} \tag{25b}$$

$$\begin{aligned} &B_{11}\frac{\partial^3 u_0}{\partial x^3} + (B_{12}+2B_{66})\frac{\partial^3 u_0}{\partial x y^2} + (B_{12}+2B_{66})\frac{\partial^3 v_0}{\partial x^2 y} + B_{22}\frac{\partial^3 v_0}{\partial y^3} \\ &-D_{11}\frac{\partial^4 w_b}{\partial x^4} - 2(D_{12}+2D_{66})\frac{\partial^4 w_b}{\partial x^2 \partial y^2} - D_{22}\frac{\partial^4 w_b}{\partial y^4} - D_{11}^s\frac{\partial^4 w_s}{\partial x^4} \\ &-2(D_{12}^s + 2D_{66}^s)\frac{\partial^4 w_s}{\partial x^2 \partial y^2} - D_{22}^s\frac{\partial^4 w_s}{\partial y^4} + q \\ &= I_0(\ddot{w}_b + \ddot{w}_s) + I_1\left(\frac{\partial \ddot{u}_0}{\partial x} + \frac{\partial \ddot{v}_0}{\partial y}\right) - I_2\nabla^2\ddot{w}_b - J_2\nabla^2\ddot{w}_s \end{aligned} \tag{25c}$$

$$\begin{aligned} &B_{11}^s\frac{\partial^3 u_0}{\partial x^3} + (B_{12}^s+2B_{66}^s)\frac{\partial^3 u_0}{\partial x \partial y^2} + (B_{12}^s+2B_{66}^s)\frac{\partial^3 v_0}{\partial x^2 \partial y} + B_{22}^s\frac{\partial^3 v_0}{\partial y^3} \\ &-D_{11}^s\frac{\partial^4 w_b}{\partial x^4} - 2(D_{12}^s+2D_{66}^s)\frac{\partial^4 w_b}{\partial x^2 \partial y^2} - D_{22}^s\frac{\partial^4 w_b}{\partial y^4} - H_{11}^s\frac{\partial^4 w_s}{\partial x^4} \\ &-2(H_{12}^s + 2H_{66}^s)\frac{\partial^4 w_s}{\partial x^2 \partial y^2} - H_{22}^s\frac{\partial^4 w_s}{\partial y^4} + A_{55}^s\frac{\partial^2 w_s}{\partial x^2} + A_{44}^s\frac{\partial^2 w_s}{\partial y^2} + q \\ &= I_0(\ddot{w}_b + \ddot{w}_s) + J_1\left(\frac{\partial \ddot{u}_0}{\partial x} + \frac{\partial \ddot{v}_0}{\partial y}\right) - J_2\nabla^2\ddot{w}_b - K_2\nabla^2\ddot{w}_s \end{aligned} \tag{25d}$$

2.6 Navier solution for simply supported rectangular sandwich plates

Rectangular plates are generally classified according to the type of support used. Here, we are concerned with the exact solutions of Eq. (25) for a simply supported FG sandwich plate. Based on the Navier approach, the solutions are assumed as

$$\begin{Bmatrix} u_0 \\ v_0 \\ w_b \\ w_s \end{Bmatrix} = \sum_{m=1}^{\infty}\sum_{n=1}^{\infty} \begin{Bmatrix} U_{mn} e^{i\omega t} \cos(\lambda x) \sin(\mu y) \\ V_{mn} e^{i\omega t} \sin(\lambda x) \cos(\mu y) \\ W_{bmn} e^{i\omega t} \sin(\lambda x) \sin(\mu y) \\ W_{smn} e^{i\omega t} \sin(\lambda x) \sin(\mu y) \end{Bmatrix} \tag{26}$$

where U_{mn}, V_{mn}, W_{bmn} and W_{smn} are arbitrary parameters to be determined, ω is the eigenfrequency associated with (m,n)th eigenmode, and $\lambda = m\pi/a$ and $\mu = n\pi/b$.

The transverse load q is also expanded in the double-Fourier sine series as

$$q(x,y) = \sum_{m=1}^{\infty}\sum_{n=1}^{\infty} q_{mn} \sin(\lambda x) \sin(\mu y) \tag{27}$$

For the case of a sinusoidally distributed load, we have

$$m = n = 1 \qquad \text{and} \qquad q_{11} = q_0 \tag{28}$$

where q_0 represents the intensity of the load at the plate centre.

Substituting Eqs. (26) and (27) into Eq. (25), the analytical solutions can be obtained from

$$\left(\begin{bmatrix} a_{11} & a_{12} & a_{13} & a_{14} \\ a_{12} & a_{22} & a_{23} & a_{24} \\ a_{13} & a_{23} & a_{33} & a_{34} \\ a_{14} & a_{24} & a_{34} & a_{44} \end{bmatrix} - \omega^2 \begin{bmatrix} m_{11} & m_{12} & m_{13} & m_{14} \\ m_{12} & m_{22} & m_{23} & m_{24} \\ m_{13} & m_{23} & m_{33} & m_{34} \\ m_{14} & m_{24} & m_{34} & m_{44} \end{bmatrix} \right) \begin{Bmatrix} U_{mn} \\ V_{mn} \\ W_{bmn} \\ W_{smn} \end{Bmatrix} = \begin{Bmatrix} 0 \\ 0 \\ q_{mn} \\ q_{mn} \end{Bmatrix} \tag{29}$$

in which

$$\begin{aligned}
a_{11} &= A_{11}\lambda^2 + A_{66}\mu^2 \\
a_{12} &= \lambda\,\mu\,(A_{12} + A_{66}) \\
a_{13} &= -\lambda\,[B_{11}\lambda^2 + (B_{12} + 2B_{66})\mu^2] \\
a_{14} &= -\lambda\,[B_{11}^s\lambda^2 + (B_{12}^s + 2B_{66}^s)\mu^2] \\
a_{22} &= A_{66}\lambda^2 + A_{22}\mu^2 \\
a_{23} &= -\mu\,[(B_{12} + 2B_{66})\lambda^2 + B_{22}\mu^2] \\
a_{24} &= -\mu\,[(B_{12}^s + 2B_{66}^s)\lambda^2 + B_{22}^s\mu^2] \\
a_{33} &= D_{11}\lambda^4 + 2(D_{12} + 2D_{66})\lambda^2\mu^2 + D_{22}\mu^4 \\
a_{34} &= D_{11}^s\lambda^4 + 2(D_{12}^s + 2D_{66}^s)\lambda^2\,\mu^2 + D_{22}^s\,\mu^4 \\
a_{44} &= H_{11}^s\lambda^4 + 2(H_{11}^s + 2H_{66}^s)\lambda^2\mu^2 + H_{22}^s\mu^4 - A_{55}^s\lambda^2 - A_{44}^s\mu^2 \\
m_{11} &= m_{22} = -I_0, \quad m_{13} = \lambda I_1, \quad m_{14} = \lambda J_1, \quad m_{23} = \mu I_1 \\
m_{24} &= \mu J_1, \quad m_{33} = -\left(I_0 + I_2(\lambda^2 + \mu^2)\right), \\
m_{34} &= -\left(I_0 + J_2(\lambda^2 + \mu^2)\right), \quad m_{44} = -\left(I_0 + K_2(\lambda^2 + \mu^2)\right),
\end{aligned} \tag{30}$$

3. Results and discussion

In this study, static and dynamic analysis of simply supported FGM sandwich plates by the present refined plate theory is suggested for investigation. Navier solutions for bending and free vibration analysis of FGM sandwich plates are presented by solving Eq. (29). A wide range of convergence and comparison studies are taken up in order to evaluate the accuracy of the formulation. Parametric studies are then carried out to investigate the effects of different geometric parameters on the static and free vibration behaviors of FGM sandwich plates and the same are discussed in subsequent sections.

3.1 Static analysis of FGM sandwich plates

Displacement and stresses obtained from the present formulation are presented for simply supported square $(a/b = 1)$ Type A and Type B FGM sandwich plates subjected to a sinusoidal transverse mechanical load $P_z = p_0\, sin\left(\frac{\pi x}{a}\right) sin\left(\frac{\pi y}{b}\right)$ applied at the top surface of the plate.

3.1.1 Sandwich plate with FGM facesheets (Type A)

Static analysis of FGM sandwich plate of Type A is discussed here. Unless mentioned otherwise, The top and bottom facesheets of the sandwich are assumed to be made of FGM with alumina at the upper surface and aluminum at the lower surface of the top facesheet and the core of the sandwich is made of pure metal i.e., aluminum and plate is symmetric about x-axis. The elastic properties of aluminum (Al) are given by $E_m = 70\, GPa,\ \rho_m = 2707\, kg/m^3$ and $\nu_m = 0.3$ and the same for alumina (Al_2O_3) are $E_c = 380\, GPa,\ \rho_c = 3800\, kg/m^3$ and $\nu_c = 0.3$.

Numerical results are presented in terms of non-dimensional stresses and deflection. The various nondimensional parameters used are

$$\overline{w} = 10\frac{E_0 h}{a^2 p_0} w\left(\frac{a}{2},\frac{b}{2},0\right); \qquad \overline{\sigma}_{xx} = \frac{10h^2}{a^2 p_0}\sigma_{xx}\left(\frac{a}{2},\frac{b}{2},\frac{h}{2}\right);$$
$$\overline{\sigma}_{yy} = \frac{10h^2}{a^2 p_0}\sigma_{yy}\left(\frac{a}{2},\frac{b}{2},\frac{h}{2}\right); \qquad \overline{\tau}_{xz} = \frac{h}{a p_0}\tau_{xz}\left(0,\frac{b}{2},0\right); \tag{31}$$
$$\overline{\tau}_{xy} = \frac{10h^2}{a^2 p_0}\tau_{xy}\left(0,0,\frac{h}{3}\right);$$

Where $E_0 = 1\, GPa$. Table 1 presents non-dimensional displacement and stresses for a 2-1-2 FGM sandwich plate obtained by present refined plate theory with the results of Shashank and Pradyumna (2018) and Neves *et al*. (2012). In this comparison study, the upper surface of top layer is made of metal (Aluminum) and bottom surface of same is made of ceramic (Zirconia, ZrO_2 having $E_c = 151\, GPa,\ \nu_c = 0.3$), the core of the sandwich is made of ceramic and the plate is symmetric about x axis. It is observed from Table 1 that the results obtained using present theory is in good agreement with those of Shashank and Pradyumna (2018) and Naves *et al*. (2012) for transverse displacement $\overline{w}$ as well as for in-plane $\overline{\sigma}_{xx}$ and transverse shear stresses $\overline{\tau}_{xz}$.

Next comparison of non-dimensional in-plane stresses $\overline{\sigma}_{xx}\left(\frac{a}{2},\frac{b}{2},\frac{z}{h}\right)$, $\overline{\sigma}_{yy}\left(\frac{a}{2},\frac{b}{2},\frac{z}{h}\right)$ and shear stress $\overline{\tau}_{xy}\left(0,0,\frac{z}{h}\right)$ through the thickness of the sandwich plate are shown in Figs. 3-5, repectively

Table 1 Non-dimensional transverse displacement and stresses of 2-1-2 sandwich plate with FGM facesheets (p = 1, a/h = 10)

Theory	$\bar{w}$	$\bar{\sigma}_{xx}$	$\bar{\tau}_{xz}$
Present	0.3062	1.4634	0.2777
Shashank and Pradyumna (2018)	0.3058	1.4806	0.2791
Naves *et al.* (2012)	0.3090	1.4742	0.2744

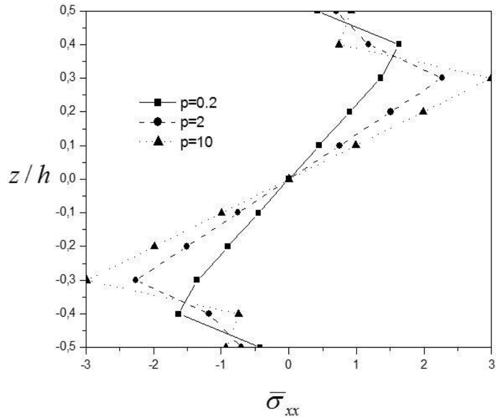

Fig. 3 Comparison of $\bar{\sigma}_{xx}$ for a simply supported 2-1-2 sandwich square plate with FGM facesheets (a/h = 10)

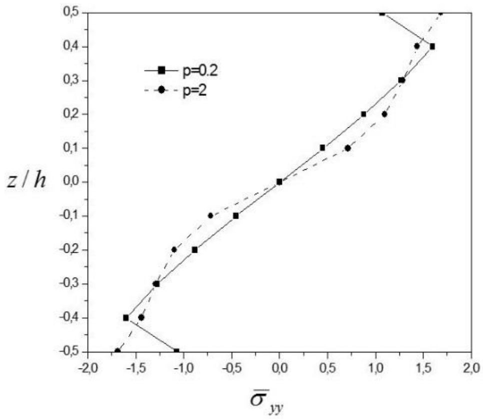

Fig. 4 Comparison of $\bar{\sigma}_{yy}$ for a simply supported 2-1-2 sandwich square plate with FGM facesheets (a/h = 10)

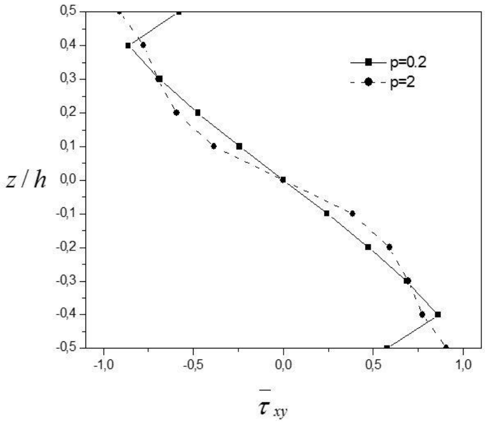

Fig. 5 Comparison of $\bar{\tau}_{xy}$ for a simply supported 2-1-2 sandwich square plate with FGM facesheets (a/h = 10)

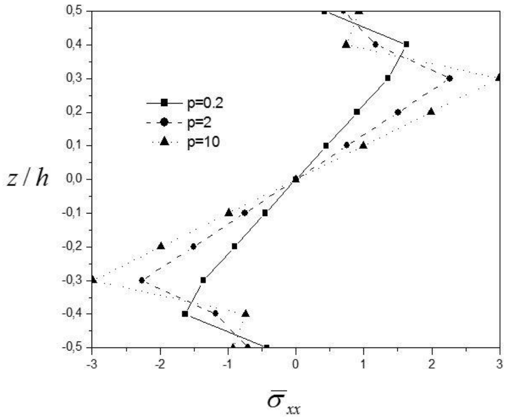

Fig. 6 Variation of $\bar{\sigma}_{xx}$ through the thickness for a simply supported 1-3-1 sandwich square plate of Type A (a/h = 10)

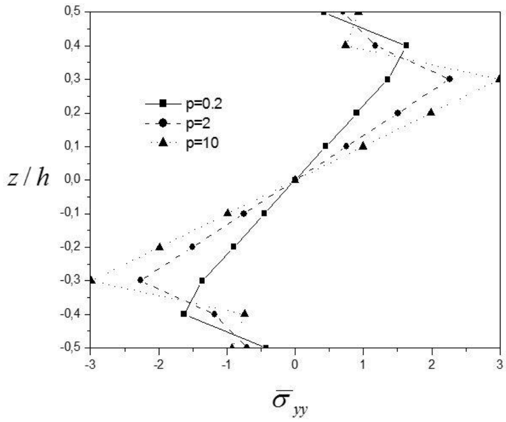

Fig. 7 Variation of $\bar{\sigma}_{yy}$ through the thickness for a simply supported 1-3-1 sandwich square plate of Type A (a/h = 10)

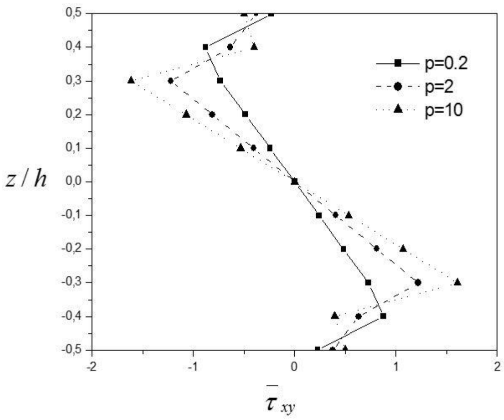

Fig. 8 Variation of $\bar{\tau}_{xy}$ through the thickness for a simply supported 1-3-1 sandwich square plate of Type A (a/h = 10)

for a 2-1-2 sandwich plate with FGM facesheets for volume fraction index (p) of 0.2 and 2. Material properties and FGM sandwich plate configuration are assumed to be same as considered in previous example. The stresses are tensile at the top surface and compressive at the bottom surface.

The variation of in-plane stresses $\bar{\sigma}_{xx}$, $\bar{\sigma}_{yy}$ and $\bar{\tau}_{xy}$ through the thickness of 1-3-1 Type A Al-Al_2O_3 FGM sandwich plate are presented in Figs. 6-8, respectively for three different volume fraction index of p = 0.2, 2 and 10. As observed from Figs. 6-8, there is a gradual variation of stresses for a volume fraction index of p = 0.2, whereas for p = 10, a sharp kink is observed at the interface. The reason for the kink in the variation of stresses is attributed to the variation of material properties along the thickness of the sandwich. For the sandwich considered in this study, a volume fraction index of p = 0.2 makes both top and bottom facesheets rich in ceramic constituent and the core is also made of same material and hence, there is a gradual variation of stresses along the thickness. For p = 10, FGM facesheets are rich in metal and the core is made of pure ceramic a mismatch of properties at the interface is leading to a sudden change of stresses, which is clearly indicated in Figs. 6-8.

3.1.2 Sandwich with FGM core (Type B)

After analyzing sandwich plate with FGM facesheets, displacement and stresses of sandwich plate with homogenous facesheets and FGM core (Type B) are studied. The plate is subjected to sinusoidal transverse mechanical load $P_z = p_0 \sin\left(\frac{\pi x}{a}\right) \sin\left(\frac{\pi y}{b}\right)$applied at the top surface of the plate. The sandwich plate has an FGM core made of Al-Al_2O_3. The top facesheet of the plate is made of alumina (Al_2O_3) and the bottom facesheet is considered to be made of aluminum (Al). First, the accuracy of the present formulation is evaluated by carrying out static analysis for a 1-8-1 Type B FGM sandwich plate. The transverse displacement and stresses are obtained for a 1-8-1 Type B FGM sandwich plate. The following non-dimensional parameters are used for transverse displacement and stresses.

$$\begin{aligned} \bar{w} &= 10\frac{E_c h^3}{a^4 p_0} w\left(\frac{a}{2},\frac{b}{2},0\right); \qquad \bar{\sigma}_{xx} = \frac{h}{a p_0}\sigma_{xx}\left(\frac{a}{2},\frac{b}{2},\frac{h}{3}\right); \\ \bar{\tau}_{xz} &= \frac{h}{a p_0}\tau_{xz}\left(0,\frac{b}{2},\frac{h}{6}\right); \qquad \bar{\tau}_{xy} = \frac{h}{a p_0}\tau_{xy}\left(0,0,\frac{h}{3}\right); \end{aligned} \tag{32}$$

Tables 2 and 3 present non-dimensional transverse displacement and stresses for FGM sandwich plate obtained by present refined theory. It is observed from Tables 2 and 3 that the results obtained by the present theory match well with those of Shashank and Pradyumna (2018), Brischetto (2009), Carrera *et al*. (2011) and Neves *et al*. (2012) for a/h ratios of 4, 10 and 100 and for two values of volume fraction index of 1 and 10 considered here.

Figs. 9-12 show the plots of variation of in-plane stresses $\bar{\sigma}_{xx}\left(\frac{a}{2},\frac{b}{2},\frac{z}{h}\right)$ and $\bar{\sigma}_{yy}\left(\frac{a}{2},\frac{b}{2},\frac{z}{h}\right)$ and transverse shear stresses $\bar{\tau}_{xz}\left(0,\frac{b}{2},\frac{z}{h}\right)$ and $\bar{\tau}_{yz}\left(\frac{a}{2},0,\frac{z}{h}\right)$ along the thickness of a 1-3-1 simply supported sandwich plate, respectively using the present theory. The FGM sandwich plate is considered to be made of Al_2O_3 and Al. $a/b = 1$ and $a/h = 100$ and the plate is subjected to a sinusoidal transverse load.

It is evident from Figs. 9 and 10 that the variation of in-plane stresses $(\bar{\sigma}_{xx}$and $\bar{\sigma}_{yy})$ along the thickness is nonlinear, since the effective Young's modulus of the core layer varies through the

Table 2 Non-dimensional transverse displacement and stresses for FGM sandwich plate of Type B (p = 1)

a/h	Theory	$\bar{w}$	$\bar{\sigma}_{xx}$	$\bar{\tau}_{xz}$	$\bar{\tau}_{xy}$
4	Present	0.7721	0.6119	0.2726	0.3295
	Shashank and Pradyumna (2018)	0.7716	0.6148	0.2701	0.3413
	Brischetto (2009)	0.7629	0.6530	–	0.3007
	Carrera *et al.* (2011)	0.7735	–	0.2596	–
	Naves *et al.* (2012)	0.7746	0.6130	0.2709	0.3301
10	Present	0.6336	1.5705	0.2738	0.8456
	Shashank and Pradyumna (2018)	0.6323	1.5661	0.2613	0.8541
	Brischetto (2009)	–	–	–	–
	Carrera *et al.* (2011)	0.6337	–	0.2593	–
	Naves *et al.* (2012)	0.6357	1.5700	0.2724	0.8453
100	Present	0.6073	15.7819	0.2740	8.4979
	Shashank and Pradyumna (2018)	0.6074	15.5157	0.2624	8.4701
	Brischetto (2009)	0.6073	15.7840	–	8.4968
	Carrera *et al.* (2011)	0.6072	–	0.2593	–
	Naves *et al.* (2012)	0.6087	15.7826	0.2743	8.4644

Table 3 Non-dimensional transverse displacement and stresses for FGM sandwich plate of Type B (p = 10)

a/h	Theory	$\bar{w}$	$\bar{\sigma}_{xx}$	$\bar{\tau}_{xz}$	$\bar{\tau}_{xy}$
4	Present	1.2216	0.3356	0.1949	0.1807
	Shashank and Pradyumna (2018)	1.2315	0.3613	0.2111	0.1832
	Brischetto (2009)	1.2232	0.3627	–	0.1412
	Carrera *et al.* (2011)	1.2240	–	0.1935	–
	Naves *et al.* (2012)	1.2183	0.3247	0.1995	0.1749
10	Present	0.8738	0.9364	0.1963	0.5041
	Shashank and Pradyumna (2018)	0.8697	0.9236	0.2135	0.5004
	Brischetto (2009)	–	–	–	–
	Carrera *et al.* (2011)	0.8743	–	0.1944	–
	Naves *et al.* (2012)	0.8712	0.9214	0.2017	0.4962
100	Present	0.8077	9.5489	0.1965	5.1417
	Shashank and Pradyumna (2018)	0.8076	9.4452	0.2125	5.0719
	Brischetto (2009)	0.8077	9.5501	–	5.1402
	Carrera *et al.* (2011)	0.8077	–	0.1946	–
	Naves *et al.* (2012)	0.8045	9.4300	0.2230	5.0672

thickness for a value of p. From Figs. 11 and 12, it is clear that the variations of non-dimensional transverse shear stresses $\bar{\tau}_{xz}$ and $\bar{\tau}_{yz}$ are parabolic in nature.

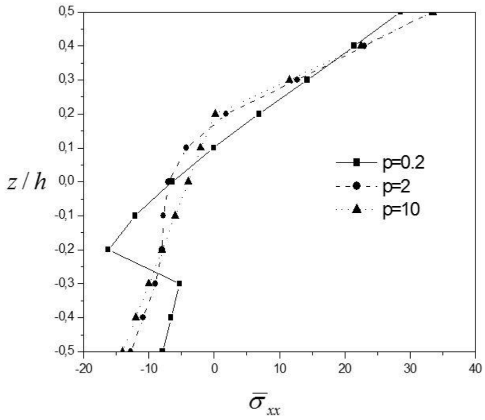

Fig. 9 Variation of $\bar{\sigma}_{xx}$ through the thickness of a simply supported 1-3-1 sandwich square plate of Type B (a/h = 100)

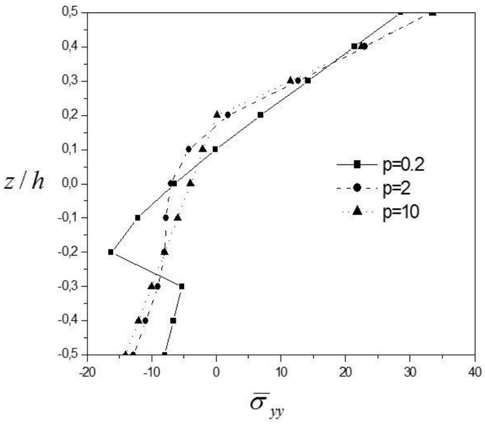

Fig. 10 Variation of $\bar{\sigma}_{yy}$ through the thickness of a simply supported 1-3-1 sandwich square plate of Type B (a/h = 100)

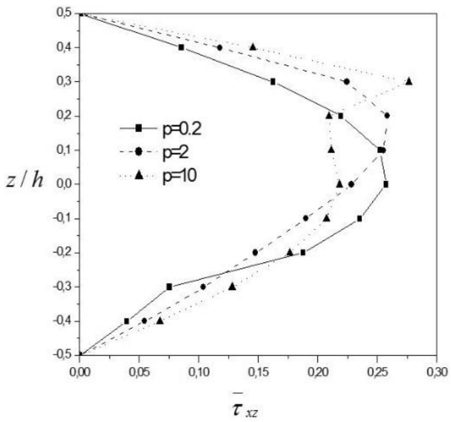

Fig. 11 Variation of $\bar{\tau}_{xz}$ through the thickness of a simply supported 1-3-1 sandwich square plate of Type B (a/h = 100)

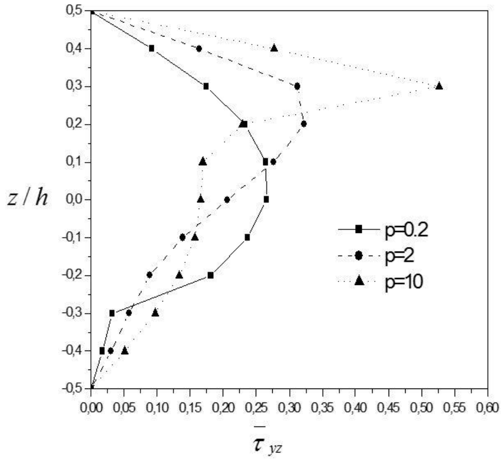

Fig. 12 Variation of $\bar{\tau}_{yz}$ through the thickness of a simply supported 1-3-1 sandwich square plate of Type B (a/h = 100)

3.2 Free vibration analysis of FGM sandwich plate

Free vibration analysis of simply supported FG sandwich plates by the present refined theory is suggested for investigation. Both Type A and Type B configurations of FGM sandwich plates, as mentioned before are considered for the investigation.

After evaluating the accuracy of the natural frequencies obtained using the present formulation, parametric study is taken up to investigate the effects of geometrical parameters and volume fraction index on the free vibration behavior of FGM sandwich plates.

First, in order to evaluate the correctness of the present theory, the non-dimensional frequencies of Al_2O_3/Al sandwich plate with FGM facesheets and homogenous core (Type A) are compared with the results of Shashank *et al*. (2018) and the three-dimensional solutions given by *Li et al*. (2008). The non-dimensional frequency parameter is considered as $\overline{\omega} = \omega(a^2/h)\sqrt{\rho_0/E_0}$ (where $\rho_0 = 1\ kg/m^3,\ E_0 = 1\ GPa$). The upper and lower surfaces of the top facesheet are rich in ceramic and metal, respectively and the core of the sandwich plate is made of pure metal (Type A). The plate is considered as symmetric about its mid-plane.

Table 4 present non-dimensional frequencies of 2-1-2, 1-1-1, 1-2-1 and 1-8-1 FGM sandwich square plate for simply supported condition, for volume fraction index p of 0.5, 1, 5 and 10 having a/h ratios 10 and 100.

It is observed from Table 4 that, volume fraction index p varying from 0.5 to 10 and a/h ratios of 10 and 100, the present theory results match well with 3D results of Li *et al*. (2008) and Shashank and Pradyumna (2018).

After establishing the correctness of the present theory, parametric studies are taken up for 1-3-1 FGM sandwich plate of Type A to study the effects of varying volume fraction index and a/h ratio on natural frequencies. It is observed from Table 5 that with increase of n from 0.5 to 10, the natural frequencies are found to be increasing as the ceramic content in FGM facesheet increases resulting in the enhancement of stiffness. Also, it is evident from Table 5 that when a/h ratio increases from 5 to 100, the natural frequencies are found to be increasing.

Table 4 Comparison of non-dimensional natural frequencies of simply supported Al_2O_3/Al sandwich plates with homogenous core and FGM facesheets (Type A)

a/h	p	Theory	2-1-2	1-1-1	1-2-1	1-8-1
10	0.5	Present	1.5273	1.4852	1.4155	1.2052
		Shashank and Pradyumna (2018)	1.5445	1.4975	1.4231	1.2072
		Li *et al.* (2008)	1.5259	1.4846	1.4166	1.2055
	1	Present	1.6811	1.6367	1.5591	1.3082
		Shashank and Pradyumna (2018)	1.6927	1.6435	1.5636	1.3086
		Li *et al.* (2008)	1.6744	1.6305	1.5579	1.3083
	5	Present	1.8387	1.8128	1.7435	1.4663
		Shashank and Pradyumna (2018)	1.8178	1.7853	1.7250	1.4643
		Li *et al.* (2008)	1.8261	1.7896	1.7267	1.4665
	10	Present	1.8496	1.8323	1.7703	1.4945
		Shashank and Pradyumna (2018)	1.8284	1.7928	1.7418	1.4915
		Li *et al.* (2008)	1.8399	1.8081	1.7481	1.4948
100	0.5	Present	1.6229	1.5817	1.5066	1.2656
		Shashank and Pradyumna (2018)	1.6317	1.5826	1.5073	1.2661
		Li *et al.* (2008)	1.6229	1.5817	1.5066	1.2656
	1	Present	1.7917	1.7538	1.6749	1.3833
		Shashank and Pradyumna (2018)	1.7926	1.7547	1.6756	1.3839
		Li *et al.* (2008)	1.7916	1.7538	1.6749	1.3833
	5	Present	1.9433	1.9365	1.8855	1.5703
		Shashank and Pradyumna (2018)	1.9439	1.9370	1.8860	1.5709
		Li *et al.* (2008)	1.9431	1.9362	1.8853	1.5704
	10	Present	1.9469	1.9508	1.9119	1.6046
		Shashank and Pradyumna (2018)	1.9475	1.9511	1.9123	1.6052
		Li *et al.* (2008)	1.9469	1.9504	1.9116	1.6046

Next, free vibration analysis of Type B FGM sandwich plate is taken up. Table 6 gives the results of 1-8-1 power-law FGM square plate of Type B. This sandwich with FGM core and homogenous facesheets is made up of alumina and aluminum. The top facesheet is rich in metal and the bottom facesheet is ceramic rich. The properties of the FGM core of the sandwich are graded between aluminum and alumina from top to bottom. The properties of the FGM core of the sandwich are graded between aluminum and alumina from top to bottom.

Table 6 present the non-dimensional frequencies $\overline{\omega} = \omega(a^2/h)\sqrt{\rho_0/E_0}$ (where $\rho_0 = 1\ kg/m^3,\ E_0 = 1\ GPa$) of simply supported FGM sandwich plates using the present theory. It is observed from Table 7 that the converged results are found to be in good agreement with the 3D results of Li *et al*. (2008) and the results of Shashank and Pradyumna (2018) for volume fraction index (p) of 0.5, 1, 5 10, a/h ratio of 10 and 100.

Next, effects of varying volume fraction index p and a/h ratios on the non-dimensional natural frequencies of 1-3-1 Type B FGM sandwich plate are studied. Table 7 presents non-

Table 5 Non-dimensional natural frequencies of simply supported 1-3-1 Al_2O_3/Al sandwich plates with homogenous core and FGM facesheets (Type A)

a/h	Theory	p				
		0.5	1	2	5	10
5	Present	1.1824	1.2756	1.3454	1.4006	1.4231
	Shashank and Pradyumna (2018)	1.1920	1.2833	1.3436	1.3786	1.3870
10	Present	1.3611	1.4965	1.6003	1.6789	1.7075
	Shashank and Pradyumna (2018)	1.3650	1.4997	1.5994	1.6688	1.6908
100	Present	1.4446	1.6043	1.7286	1.8215	1.8535
	Shashank and Pradyumna (2018)	1.4453	1.6050	1.7293	1.8221	1.8540

Table 6 Non-dimensional natural frequencies of simply supported 1-8-1 Al_2O_3/Al sandwich plate with FGM core

a/h	p	Li *et al.* (2008)	Shashank and Pradyumna (2018)	Present
10	0.5	1.2975	1.3009	1.2946
	1	1.3485	1.3510	1.3454
	5	1.4931	1.4945	1.4905
	10	1.5498	1.5517	1.5476
100	0.5	1.3393	1.3558	1.3393
	1	1.3867	1.4048	1.3867
	5	1.5314	1.5504	1.5314
	10	1.5911	1.6018	1.5910

Table 7 Non-dimensional natural frequencies of simply supported 1-3-1 Al_2O_3/Al sandwich plates with FGM core and homogenous facesheets (Type B)

a/h	Theory	p				
		0.5	1	2	5	10
5	Present	1.2677	1.2038	1.1475	1.1070	1.0940
	Shashank and Pradyumna (2018)	1.2727	1.2095	1.1551	1.1176	1.1032
10	Present	1.3624	1.2984	1.2473	1.2228	1.2216
	Shashank and Pradyumna (2018)	1.3644	1.3007	1.2504	1.2271	1.2254
100	Present	1.4002	1.3365	1.2884	1.2726	1.2777
	Shashank and Pradyumna (2018)	1.4009	1.3374	1.2894	1.2737	1.2698

dimensional natural frequencies of simply supported 1-3-1 Al_2O_3/Al FGM sandwich plate for five different values of volume fraction index p of 0.5, 1, 2, 5 and 10 and a/h ratios of 5, 10 and 100. It is observed from Table 8 that for a particular a/h ratio, non-dimensional natural frequencies are found to be decreasing when the value of p is increased from 0.5 to 10. This behavior is expected, as with increase in p from 0.5 to 10, the FGM core becomes metal rich resulting in the reduction of stiffness leading to decrease of frequency. Also, for a particular value of volume fraction index (p) the non-dimensional natural frequencies are found to be increasing when a/h ratio changes from 5 to 100.

4. Conclusions

In this present study, a refined shear deformation plate theory is employed to investigate the bending and free vibration problems of two types of FGM sandwich plates. Numerical examples were performed on simply supported sandwich plates, made of functionally graded materials in the core or in the skins, for various material power-law exponents and side to-thickness and skin-core-skin thickness ratios. Obtained results were presented in figures and tables and compared with references and these demonstrate the accuracy of present approach. It can be said that the present refined plate theory is much simpler, straightforward and can be easily applied for wide range of problems for static and free vibration analyses of FGM sandwich plates and the same is recommended for analyses of FGM sandwich plates.

References

Abazid, A., Alotebi, M.S. and Sobhy, M. (2018), "A novel shear and normal deformation theory for hygrothermal bending response of FGM Sandwich plates on Pasternak elastic foundation", *Struct. Eng. Mech., Int. J.*, **67**(3), 219-232. https://doi.org/10.12989/sem.2018.67.3.219

Abdelaziz, H.H., Ait Amar Meziane M., Bousahla, A.A., Tounsi, A., Mahmoud, S.R. and Alwabli, A.S. (2017), "An efficient hyperbolic shear deformation theory for bending, buckling and free vibration of FGM sandwich plates with various boundary conditions", *Steel Compos. Struct., Int. J.*, **25**(6), 693-704. https://doi.org/10.12989/scs.2017.25.6.693

Abualnour, M., Chikh, A., Hebali, H., Kaci, A., Tounsi, A., Bousahla, A.A. and Tounsi, A. (2019), "Thermomechanical analysis of antisymmetric laminated reinforced composite plates using a new four variable trigonometric refined plate theory", *Comput. Concrete, Int. J.*, **24**(6), 489-498. https://doi.org/10.12989/cac.2019.24.6.489

Adda Bedia, W., Houari, M.S.A., Bessaim, A., Bousahla, A.A., Tounsi, A., Saeed, T. and Alhodaly, M.S. (2019), "A new hyperbolic two-unknown beam model for bending and buckling analysis of a nonlocal strain gradient nanobeams", *J. Nano Res.*, **57**, 175-191. https://doi.org/10.4028/www.scientific.net/JNanoR.57.175

Addou, F.Y., Meradjah, M., Bousahla, A.A., Benachour, A., Bourada, F., Tounsi, A. and Mahmoud, S.R. (2019), "Influences of porosity on dynamic response of FG plates resting on Winkler/Pasternak/Kerr foundation using quasi 3D HSDT", *Comput. Concrete, Int. J.*, **24**(4), 347-367. https://doi.org/10.12989/cac.2019.24.4.347

Ahmadi, I. (2018), "Three-dimensional and free-edge hygrothermal stresses in general long Sandwich plates", *Struct. Eng. Mech., Int. J.*, **65**(3), 275-290. https://doi.org/10.12989/sem.2018.65.3.275

Akbaş, Ş.D. (2015a), "Wave propagation of a functionally graded beam in thermal environments", *Steel Compos. Struct., Int. J.*, **19**(6), 1421-1447. https://doi.org/10.12989/scs.2015.19.6.1421

Akbaş, Ş.D. (2015b), "Free vibration and bending of functionally graded beams resting on elastic foundation", *Res. Eng. Struct. Mater.*, **1**(1), 25-37. http://dx.doi.org/10.17515/resm2015.03st0107

Akbaş, Ş.D. (2015c), "Post-buckling analysis of axially functionally graded three-dimensional beams", *Int. J. Appl. Mech.*, **7**(3), 1550047. https://doi.org/10.1142/S1758825115500477

Akbaş, Ş.D. (2017a), "Vibration and static analysis of functionally graded porous plates", *J. Appl. Computat. Mech.*, **3**(3), 199-207. https://doi.org/10.22055/JACM.2017.21540.1107

Akbaş, Ş.D. (2017b), "Stability of a non-homogenous porous plate by using generalized differantial quadrature method”, *Int. J. Eng. Appl. Sci.*, **9**, 147-155. https://doi.org/10.24107/ijeas.322375

Akbaş, Ş.D. (2017c), “Nonlinear static analysis of functionally graded porous beams under thermal effect”, *Coupl. Syst. Mech., Int. J.*, **6**(4), 399-415. https://doi.org/10.12989/csm.2017.6.4.399

Akbaş, Ş.D. (2017d), “Forced vibration analysis of functionally graded nanobeams”, *Int. J. Appl. Mech.*, **9**(7), 1750100. https://doi.org/10.1142/S1758825117501009

Akbaş, Ş.D. (2018), “Geometrically nonlinear analysis of functionally graded porous beams”, *Wind Struct., Int. J.*, **27**(1), 59-70. https://doi.org/10.12989/was.2018.27.1.059

Akbaş, Ş.D. (2019), “Forced vibration analysis of functionally graded sandwich deep beams”, *Coupl. Syst. Mech., Int. J.*, **8**(3), 259-271. https://doi.org/10.12989/csm.2019.8.3.259

Alimirzaei, S., Mohammadimehr, M. and Tounsi, A. (2019), “Nonlinear analysis of viscoelastic micro-composite beam with geometrical imperfection using FEM: MSGT electro-magneto-elastic bending, buckling and vibration solutions”, *Struct. Eng. Mech., Int. J.*, **71**(5), 485-502. https://doi.org/10.12989/sem.2019.71.5.485

Amirani, M.C., Khalili, S.M.R. and Nemati, N. (2009), “Free vibration analysis of sandwich beam with FG core using the element free Galerkin method”, *Compos. Struct.*, **90**(3), 373-379. https://doi.org/10.1016/j.compstruct.2009.03.023

Arani, A.G., Maraghi Z.K. and Ferasatmanesh, M. (2017), “Theoretical investigation on vibration frequency of sandwich plate with PFRC core and piezomagnetic face sheets under variable in-plane load”, *Struct. Eng. Mech., Int. J.*, **63**(1), 65-76. https://doi.org/10.12989/sem.2017.63.1.065

Balubaid, M., Tounsi, A., Dakhel, B. and Mahmoud, S.R. (2019), “Free vibration investigation of FG nanoscale plate using nonlocal two variables integral refined plate theory”, *Comput. Concrete, Int. J.*, **24**(6), 579-586. https://doi.org/10.12989/cac.2019.24.6.579

Belarbi, M.O., Tati, A., Ounis, H. and Benchabane, A. (2016), “Development of a 2D isoparametric finite element model based on the layerwise approach for the Bending analysis of sandwich plates”, *Struct. Eng. Mech., Int. J.*, **57**(3), 473-506. https://doi.org/10.12989/sem.2016.57.3.473

Belbachir, N., Draiche, K., Bousahla, A.A., Bourada, M., Tounsi, A. and Mahmoud, S.R. (2019), “Bending analysis of anti-symmetric cross-ply laminated plates under nonlinear thermal and mechanical loadings”, *Steel Compos. Struct., Int. J.*, **33**(1), 913-924. https://doi.org/10.12989/scs.2019.33.1.081

Berghouti, H., Adda Bedia, E.A., Benkhedda, A. and Tounsi, A. (2019), “Vibration analysis of nonlocal porous nanobeams made of functionally graded material”, *Adv. Nano Res., Int. J.*, **7**(5), 351-364. https://doi.org/10.12989/anr.2019.7.5.351

Boukhlif, Z., Bouremana, M., Bourada, F., Bousahla, A.A., Bourada, M., Tounsi, A. and Al-Osta, M.A. (2019), “A simple quasi-3D HSDT for the dynamics analysis of FG thick plate on elastic foundation”, *Steel Compos. Struct., Int. J.*, **31**(5), 503-516. https://doi.org/10.12989/scs.2019.31.5.503

Boulefrakh, L., Hebali, H., Chikh, A., Bousahla, A.A., Tounsi, A. and Mahmoud, S.R. (2019), “The effect of parameters of visco-Pasternak foundation on the bending and vibration properties of a thick FG plate”, *Geomech. Eng., Int. J.*, **18**(2), 161-178. https://doi.org/10.12989/gae.2019.18.2.161

Bourada, F., Bousahla, A.A., Bourada, M., Azzaz, A., Zinata, A. and Tounsi, A. (2019), “Dynamic investigation of porous functionally graded beam using a sinusoidal shear deformation theory”, *Wind Struct., Int. J.*, **28**(1), 19-30. https://doi.org/10.12989/was.2019.28.1.019

Boussoula, A., Boucham, B., Bourada, M., Bourada, F., Tounsi, A., Bousahla, A.A. and Tounsi, A. (2020), “A simple nth-order shear deformation theory for thermomechanical bending analysis of different configurations of FG sandwich plates”, *Smart Struct. Syst., Int. J.*, **25**(2), 195-216. https://doi.org/10.12989/sss.2020.25.2.195

Boutaleb, S., Benrahou, K.H., Bakora, A., Algarni, A., Bousahla, A.A., Tounsi, A., Tounsi, A. and Mahmoud, S.R. (2019), “Dynamic Analysis of nanosize FG rectangular plates based on simple nonlocal quasi 3D HSDT”, *Adv. Nano Res., Int. J.*, **7**(3), 189-206. https://doi.org/10.12989/anr.2019.7.3.191

Brischetto, S. (2009), “Classical and mixed advanced models for sandwich plates embedding functionally graded cores”, *J. Mech. Mater. Struct.*, **4**(1), 13-33. https://doi.org/10.2140/jomms.2009.4.13

Carrera, E., Brischetto, S., Cinefra, M. and Soave, M. (2011), “Effects of thickness stretching in functionally graded plates and shells”, *Compos. B Eng.*, **42**(2), 123-133.

https://doi.org/10.1016/j.compositesb.2010.10.005
Chaabane, L.A., Bourada, F., Sekkal, M., Zerouati, S., Zaoui, F.Z., Tounsi, A., Derras, A., Bousahla, A.A. and Tounsi, A. (2019), "Analytical study of bending and free vibration responses of functionally graded beams resting on elastic foundation", *Struct. Eng. Mech., Int. J.*, **71**(2), 185-196. https://doi.org/10.12989/sem.2019.71.2.185
Cunedioglu, Y. (2015), "Free vibration analysis of edge cracked symmetric functionally graded sandwich beams", *Struct. Eng. Mech., Int. J.*, **56**(6), 1003-1020. https://doi.org/10.12989/sem.2015.56.6.1003
Dash, S., Mehar, K., Sharma, N., Mahapatra, T.R. and Panda, S.K. (2018), "Modal analysis of FG sandwich doubly curved shell structure", *Struct. Eng. Mech., Int. J.*, **68**(6), 721-733. https://doi.org/10.12989/sem.2018.68.6.721
Draiche, K., Bousahla, A.A., Tounsi, A., Alwabli, A.S., Tounsi, A. and Mahmoud, S.R. (2019), "Static analysis of laminated reinforced composite plates using a simple first-order shear deformation theory", *Comput. Concrete, Int. J.*, **24**(4), 369-378. https://doi.org/10.12989/cac.2019.24.4.369
Draoui, A., Zidour, M., Tounsi, A. and Adim, B. (2019), "Static and dynamic behavior of nanotubes-reinforced sandwich plates using (FSDT)", *J. Nano Res.*, **57**, 117-135. https://doi.org/10.4028/www.scientific.net/JNanoR.57.117
Hellal, H., Bourada, M., Hebali, H., Bourda, F., Tounsi, A., Bousahla, A.A. and Mahmour, S.R. (2019), "Dynamic and stability analysis of functionally graded material sandwich plates in hygro-thermal environment using a simple higher shear deformation theory", *J. Sandw. Struct. Mater.* https://doi.org/10.1177/1099636219845841
Hussain, M., Naeem, M.N., Tounsi, A. and Taj, M. (2019), "Nonlocal effect on the vibration of armchair and zigzag SWCNTs with bending rigidity", *Adv. Nano Res., Int. J.*, **7**(6), 431-442. https://doi.org/10.12989/anr.2019.7.6.431
Kaddari, M., Kaci, A., Bousahla, A.A., Tounsi, A., Bourada, F., Tounsi, A., Adda Bedia, E.A. and Al-Osta, M.A. (2020), "A study on the structural behaviour of functionally graded porous plates on elastic foundation using a new quasi-3D model: Bending and Free vibration analysis", *Comput. Concrete, Int. J.*, **25**(1), 37-57. https://doi.org/10.12989/cac.2020.25.1.037
Karami, B., Janghorban, M. and Tounsi, A. (2019a), "Galerkin's approach for buckling analysis of functionally graded anisotropic nanoplates/different boundary conditions", *Eng. Comput.*, **35**, 1297-1316. https://doi.org/10.1007/s00366-018-0664-9
Karami, B., Janghorban, M. and Tounsi, A. (2019b), "Wave propagation of functionally graded anisotropic nanoplates resting on Winkler-Pasternak foundation", *Struct. Eng. Mech., Int. J.*, **7**(1), 55-66. https://doi.org/10.12989/sem.2019.70.1.055
Karami, B., Shahsavari, D., Janghorban, M. and Tounsi, A. (2019c), "Resonance behavior of functionally graded polymer composite nanoplates reinforced with grapheme nanoplatelets", *Int. J. Mech. Sci.*, **156**, 94-105. https://doi.org/10.1016/j.ijmecsci.2019.03.036
Karami, B., Janghorban, M. and Tounsi, A. (2019d), "On exact wave propagation analysis of triclinic material using three dimensional bi-Helmholtz gradient plate model", *Struct. Eng. Mech., Int. J.*, **69**(5), 487-497. https://doi.org/10.12989/sem.2019.69.5.487
Karami, B., Janghorban, M. and Tounsi, A. (2019e), "On pre-stressed functionally graded anisotropic nanoshell in magnetic field", *J. Brazil. Soc. Mech. Sci. Eng.*, **41**(11), 495. https://doi.org/10.1007/s40430-019-1996-0
Khiloun, M., Bousahla, A.A., Kaci, A., Bessaim, A., Tounsi, A. and Mahmoud, S.R. (2019), "Analytical modeling of bending and vibration of thick advanced composite plates using a four-variable quasi 3D HSDT", *Eng. Comput.* https://doi.org/10.1007/s00366-019-00732-1
Kolahdouzan, F., Arani, A.G. and Abdollahian, M. (2018), "Buckling and free vibration analysis of FG-CNTRC-micro sandwich plate", *Steel Compos. Struct., Int. J.*, **26**(3), 273-287. https://doi.org/10.12989/scs.2018.26.3.273
Li, Q., Iu, V.P. and Kou, K.P. (2008), "Three-dimensional vibration analysis of functionally graded material sandwich plates", *J. Sound Vib.*, **311**, 498-515. https://doi.org/10.1016/j.jsv.2007.09.018
Mahmoudi, A., Benyoucef, S., Tounsi, A., Benacour, A., Adda Bedia, E.A. and Mahmoud, S.R. (2019), "A

refined quasi-3D shear deformation theory for thermo-mechanical behavior of functionally graded sandwich plates on elastic foundations”, *J. Sandw. Struct. Mater.*, **21**(6), 1906-1926. https://doi.org/10.1177/1099636217727577

Medani, M., Benahmed, A., Zidour, M., Heireche, H., Tounsi, A., Bousahla, A.A., Tounsi, A. and Mahmoud, S.R. (2019), “Static and dynamic behavior of (FG-CNT) reinforced porous sandwich plate”, *Steel Compos. Struct., Int. J.*, **32**(5), 595-610. https://doi.org/10.12989/scs.2019.32.5.595

Mekerbi, M., Benyoucef, S., Mahmoudi, A., Tounsi, A., Bousahla, A.A. and Mahmoud, S.R. (2019), “Thermodynamic behavior of functionally graded sandwich plates resting on different elastic foundation and with various boundary conditions”, *J. Sandw. Struct. Mater.*, 1-30. https://doi.org/10.1177/1099636219851281

Meksi, R., Benyoucef, S., Mahmoudi, A., Tounsi, A., Adda Bedia, E.A. and Mahmoud, S.R. (2019), “An analytical solution for bending, buckling and vibration responses of FGM sandwich plates”, *J. Sandw. Struct. Mater.*, **21**(2), 727-757. https://doi.org/10.1177/1099636217698443

Mirza, S.B., Hussain Khan, A. and Yasin, Y. (2018), “Effect of boundary conditions on the non-linear forced vibration response of isotropic plates”, *IOP Conference Series: Mater. Sci. Eng.*, **377**, 012089. https://doi.org/10.1088/1757-899X/377/1/012089

Nazargah, M.L. and Meshkani, Z. (2018), “An efficient partial mixed finite element model for static and free vibration analyses of FGM plates rested on two-parameter elastic foundations”, *Struct. Eng. Mech., Int. J.*, **66**(5), 665-676. https://doi.org/10.12989/sem.2018.66.5.665

Neves, A.M.A., Ferreira, A.J.M., Carrera, E., Cinefra, M., Jorge, R.M.N. and Soares, C.M.M. (2012), “Static analysis of functionally graded sandwich plates according to a hyperbolic theory considering Zig-Zag and warping effects”, *Adv. Eng. Software*, **52**, 30-43. https://doi.org/10.1016/j.advengsoft.2012.05.005

Sahla, M., Saidi, H., Draiche, K., Bousahla, A.A., Bourada, F. and Tounsi, A. (2019), “Free vibration analysis of angle-ply laminated composite and soft core sandwich plates”, *Steel Compos. Struct., Int. J.*, **33**(5), 663-679. https://doi.org/10.12989/scs.2019.33.5.663

Semmah, A., Heireche, H., Bousahla, A.A. and Tounsi, A. (2019), “Thermal buckling analysis of SWBNNT on Winkler foundation by non local FSDT”, *Adv. Nano Res., Int. J.*, **7**(2), 89-98. https://doi.org/10.12989/anr.2019.7.2.089

Shashank, P. and Pradyumna, S. (2018), “Analysis of functionally graded sandwich plates using a higher-order layerwise theory”, *Compos. Part B*, **153**, 325-336. https://doi.org/10.1016/j.compositesb.2018.08.121

Sudhakar, V., Gopalkrishnan, S. and Vijayaraju, K. (2018), “Development of super convergent euler finite elements for the analysis of sandwich beams with soft core”, *Struct. Eng. Mech., Int. J.*, **65**(6), 657-678. https://doi.org/10.12989/sem.2018.65.6.657

Thai, C.H., Zenkour, A.M., Wahab, M.A. and Nguyen-Xuan, H. (2016), “A simple four-unknown shear and normal deformations theory for functionally graded isotropic and sandwich plates based on isogeometric analysis”, *Compos. Struct.*, **139**, 77-95. https://doi.org/10.1016/j.compstruct.2015.11.066

Tlidji, Y., Zidour, M., Draiche, K., Safa, A., Bourada, M., Tounsi, A., Bousahla, A.A. and Mahmoud, S.R. (2019), “Vibration analysis of different material distributions of functionally graded microbeam”, *Struct. Eng. Mech., Int. J.*, **69**(6), 637-649. https://doi.org/10.12989/sem.2019.69.6.637

Zaoui, F.Z., Ouinas, D. and Tounsi, A. (2019), “New 2D and quasi-3D shear deformation theories for free vibration of functionally graded plates on elastic foundations”, *Compos. Part B*, **159**, 231-247. https://doi.org/10.1016/j.compositesb.2018.09.051

Zarga, D., Tounsi, A., Bousahla, A.A., Bourada, F. and Mahmoud, S.R. (2019), “Thermomechanical bending study for functionally graded sandwich plates using a simple quasi-3D shear deformation theory”, *Steel Compos. Struct., Int. J.*, **32**(3), 389-410. https://doi.org/10.12989/scs.2019.32.3.389

Zenkour, A.M. (2005), “A comprehensive analysis of functionally graded sandwich plates: Part 1-deflection and stresses”, *Int. J. Solid Struct.*, **42**(18-19), 5224-5242. https://doi.org/10.1016/j.ijsolstr.2005.02.015

Zenkour, A.M. and Alghamdi, N.A. (2008), “Thermoelastic bending analysis of functionally graded sandwich plates”, *J. Mater. Sci.*, **43**(8), 2574-2589. https://doi.org/10.1007/s10853-008-2476-6

CC